

Pair-breaking critical current density of magnesium diboride

Milind N. Kunchur*

Department of Physics and Astronomy, University of South Carolina, Columbia, South Carolina 29208, USA

Sung-Ik Lee and W. N. Kang

Department of Physics, Pohang University of Science and Technology, Pohang 790-784, Republic of Korea

(Received 28 May 2003; published 27 August 2003)

We report the investigation of the pair-breaking current density j_d in magnesium diboride. At low current densities j , the transition temperature T_c shifts in the classic $\Delta T_c(j)/T_c(0) \propto -[j/j_d(0)]^{2/3}$ manner, with a projected $j_d(0) \approx 2 \times 10^7$ A/cm². Current-voltage curves at fixed temperatures yield a similar value for $j_d(0)$, with an overall $j_d(T)$ dependence consistent with Ginzburg-Landau theory. To our knowledge this is the first complete investigation of $j_d(T)$ down to $T \approx 0$ in any superconductor.

DOI: 10.1103/PhysRevB.68.064516

PACS number(s): 74.25.Sv, 74.25.Bt, 74.25.Fy

I. INTRODUCTION

Magnesium diboride (MgB₂) recently made an impact as a promising new superconductor with a surprisingly high critical temperature for a simple binary compound. This has spurred considerable research activity into investigating the myriad properties associated with its superconducting state. Besides the critical temperature T_c and the upper critical field H_{c2} , an intrinsic parameter that sets a fundamental limit to the survival of superconductivity is the pair-breaking (or depairing) critical current density j_d . We obtain an estimate of this important quantity in the MgB₂ superconductor, which sets an absolute limit to the maximum current-carrying performance under ideal conditions. This also represents, to our knowledge, the only complete ($0 \leq T \leq T_c$) investigation of j_d by a direct transport method in any superconductor.

When a superconducting state is formed, charge carriers correlate and condense into a coherent macroscopic quantum state. The formation of this state is governed principally by a competition between four energies: condensation, magnetic-field expulsion, thermal, and kinetic. The order parameter Δ , which describes the extent of condensation and the strength of the superconducting state, is reduced as the temperature T , magnetic field H , and electric current density j are increased. The boundary in the T - H - j phase space, which separates the superconducting and normal states, is where Δ vanishes, and the three parameters attain their critical values $T_c(H, j)$, $H_{c2}(T, j)$, and $j_d(T, H)$.

In practice, a superconductor loses its ability to carry dissipationless current long before j reaches j_d . Any process that causes the phase difference between two points to change with time—such as the motion of flux vortices, phase slip centers in narrow wires, junctions, and fluctuations—can generate a finite voltage and hence resistance. The conventional critical-current density j_c that marks this onset of dissipation can be much lower than j_d . In the highly dissipative regime between j_c and j_d , the principle of minimum entropy production ensures a homogeneous current flow, but attaining j_d is usually preceded by heating at contacts and within the bulk of the sample. On the other hand, a measurement of j_d in low- T_c type-I superconductors is complicated by the

low T_c 's (hence much lower tolerance for heating), Silsbee's rule, and the Meissner effect which concentrates the current flow near the surface (unless the dimensions are sufficiently small). These technical obstacles have previously prevented a measurement of the full $j_d(T)$ function down to $T \approx 0$.

The success of the present work became feasible because of four favorable factors: MgB₂ has a high T_c comparable to cuprates (so for a given Joule heating the fractional T error is small). On the other hand, its normal resistivity ρ_n is $\sim 1/100$ and its j_d is $\sim 1/10$ that of cuprates, which reduce the Joule power density ρj^2 by three orders of magnitude. Finally, we use a highly evolved pulsed-current technique (which we have refined over ten years) to further reduce heating to negligible levels, permitting a measurement of $j_d(T)$ at all T .

II. THEORETICAL BACKGROUND

A theoretical estimate of j_d can be obtained from the Ginzburg-Landau (GL) theory, in which the strength of the superconducting state is expressed through the complex phenomenological order parameter $\psi = |\psi|e^{i\varphi}$. The superfluid density near T_c is proportional to $|\psi|^2$ and the free-energy density f of the system (with respect to the free-energy density in the normal state) can be expressed as a power expansion in $|\psi|^2$ (In "dirty" superconductors—superconductors with a high impurity scattering rate—the approximate validity of the GL expressions extends down to $T \ll T_c$.) In the absence of significant magnetic fields and in situations where the magnitude of the order parameter $|\psi|$ is uniform (either because the dimensions of the sample are small compared to the coherence length or because of the principle of minimum entropy production at high dissipation levels¹) f can be expressed as²

$$f = \alpha |\psi|^2 + \frac{\beta}{2} |\psi|^4 + \frac{1}{2} |\psi|^2 m^* v_s^2. \quad (1)$$

α and β are negative and positive constants, respectively (α becomes positive above T_c), and the positive third term is the kinetic-energy density expressed in terms of the superfluid velocity $\mathbf{v}_s = \hbar \nabla \varphi / m^* - e^* \mathbf{A} / cm^*$; where e^* and m^* are, respectively, the effective charge and mass of a Cooper

pair. For zero v_s , the equilibrium value of $|\psi|^2$ that minimizes the free energy [Eq. (1)] is $|\psi_\infty|^2 = -\alpha/\beta$. For a finite v_s it becomes

$$|\psi|^2 = |\psi_\infty|^2 \left(1 - \frac{m^* v_s^2}{2|\alpha|} \right). \quad (2)$$

The corresponding supercurrent density is

$$j = e^* |\psi|^2 v_s = 2e |\psi_\infty|^2 \left(1 - \frac{m^* v_s^2}{2|\alpha|} \right) v_s. \quad (3)$$

The maximum possible value of this expression can now be identified with j_d ,

$$j_d(T) = 2e |\psi_\infty|^2 \frac{2}{3} \left(\frac{2\alpha}{3m^*} \right)^{1/2} = \frac{cH_c(T)}{3\sqrt{6}\pi\lambda(T)}, \quad (4)$$

where the GL-theory parameters were replaced by their expressions $\alpha(T) = -(e^*2/m^*c^2)H_c^2(T)\lambda^2(T)$ and $\beta(T) = (4\pi e^*4/m^*c^4)H_c^2(T)\lambda^4(T)$ in terms of the physically measurable quantities H_c (thermodynamic critical field) and λ (magnetic penetration depth). The relations $H_c(T) \approx H_c(0)[1 - (T/T_c)^2]$ and $\lambda(T) \approx \lambda(0)/\sqrt{[1 - (T/T_c)^4]}$ give

$$j_d(T) \approx j_d(0)[1 - (T/T_c)^2]^{3/2}[1 + (T/T_c)^2]^{1/2}, \quad (5)$$

where

$$j_d(0) = cH_c(0)/[3\sqrt{6}\pi\lambda(0)] \quad (6)$$

is the zero-temperature depairing current density. Close to T_c , Eq. (5) reduces to $j_d(T \approx T_c) \approx 4j_d(0)[1 - T/T_c]^{3/2}$. This can be inverted to give the shift in transition temperature $T_c(j)$ at small currents, with the well-known $j^{2/3}$ proportionality:

$$\frac{T_c(0) - T_c(j)}{T_c(0)} \approx \left(\frac{1}{4} \right)^{2/3} \left[\frac{j}{j_d(0)} \right]^{2/3}. \quad (7)$$

(The preceding discussion is based on Refs. 2 and 3.) Note that if heat removal from the sample is ineffective, Joule heating will give an apparent shift $\Delta T_c \propto \rho j^2$, which is the cube of the intrinsic $\sim j^{2/3}$ depairing shift near T_c , and hence easily distinguishable.

III. EXPERIMENTAL DETAILS

The samples are 400-nm-thick films of MgB_2 fabricated using a two-step method whose details are described elsewhere.^{4,5} An amorphous boron film was deposited on a (1 $\bar{1}$ 02) Al_2O_3 substrate at room temperature by pulsed-laser ablation. The boron film was then put into a Nb tube with high-purity Mg metal (99.9%) and the Nb tube was then sealed using an arc furnace in an argon atmosphere. Finally, the heat treatment was carried out at 900 °C for 30 min in an evacuated quartz ampoule sealed under high vacuum. X-ray diffraction indicates a highly c -axis-oriented crystal structure normal to the substrate with undetectable ($<0.1\%$) impurity phases. Magnetization $M(T)$ curves have a λ -limited transition width of 1.5 K (T_c spread <0.2 K). However, varia-

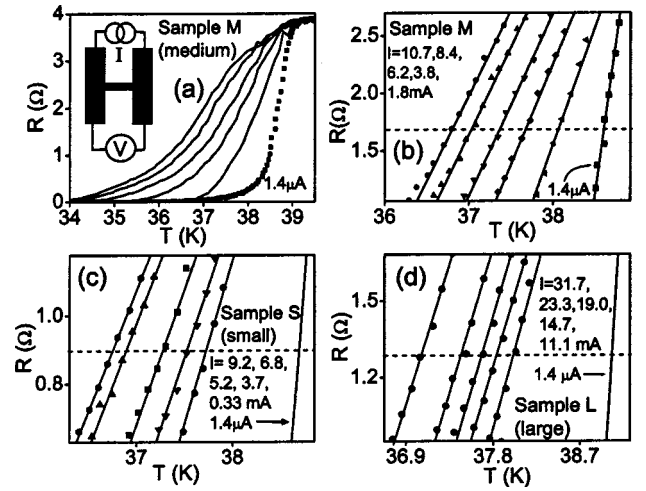


FIG. 1. Resistive transitions of MgB_2 bridges at different currents (values correspond to curves from left to right). Panels (a) and (b) show two windows of the same data. The inset in (a) shows the sample geometry and configuration of leads. Panels (b–d) show the central main portions of the transitions for three different sized samples. The rightmost curves at $I = 1.4 \mu\text{A}$ were measured with a continuous dc current; the rest used pulsed signals. The dashed lines represents $R = R_n/2$ for each sample.

tions in thickness ($\delta t/t \sim 10\%$) produce a slight broadening of $R(T)$ with increasing j . The films were photolithographically patterned down to narrow bridges. In this paper we show data on three bridges, labeled S, M, and L (for small, medium, and large) with lateral dimensions 2.8×33 , 3.0×61 , and $9.7 \times 172 \mu\text{m}^2$, respectively. The lateral dimensions are uncertain by $\pm 0.7 \mu\text{m}$ and the mean thickness by ± 50 nm.

The electrical transport measurements were made using a pulsed signal source. Pulse durations range 0.1–4 μs with a duty cycle of about 1 ppm. About 100 pulses are averaged to yield low-noise data as exemplified in Fig. 1. Pulse waveforms under worst conditions (high I and R) are shown in Fig. 2(b). $R(t) = V(t)/I(t)$ has a 50 ns rise time. From past experience with other films (e.g., $\text{Y}_1\text{Ba}_2\text{Cu}_3\text{O}_7$ on LaAlO_3 where detailed information on thermal constants allows a first-principles calculation), we found that micrometer-wide bridges typically have thermal resistances of order R_{th}

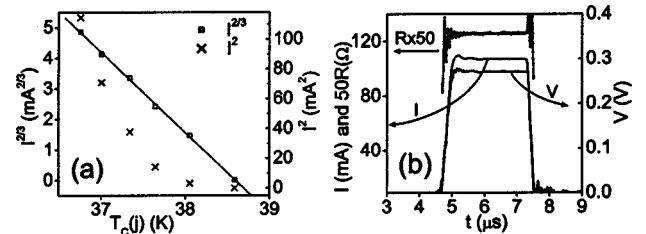


FIG. 2. (a) Shifted transition temperatures at different currents. The two y axes plot the same $T_c(j)$ data vs $I^{2/3}$ and I^2 , showing adherence to the $I^{2/3}$ law for pair breaking rather than the I^2 law for Joule heating. The linear fit (solid line) to the $I^{2/3}$ plot gives $I_d(0) = 257$ mA [see Eq. (7)]. (b) Pulse waveforms at $j = 9.7$ MA/cm², $E = 83$ V/cm, and power density $jE = 803$ MW/cm³.

$\sim 1\text{--}10\text{ nK cm}^3/\text{W}$ at μs time scales.^{6,17} Additionally, the absence of sample heating was ascertained by repeating the measurement in different thermal environments (see below). Contact resistances are much less than the normal resistance R_n of the bridge; heat generated there does not interfere with the bridge since the thermal diffusion distance ($\sqrt{Dt} \sim 10\ \mu\text{m}$) is much shorter than the contact-to-bridge distance ($>1\ \text{mm}$). All measurements were made in zero applied magnetic field with a worst case self-field at a bridge's edge of $\sim 300\ \text{G}$. Thus resistance from flux flow $R_f \sim R_n B/H_{c2}$ is a small fraction ($<5\%$) of R_n . Hence we are not merely measuring a depinning j_c ; without significant pair breaking (or gross heating) flux motion above j_c will give $R_f \ll R_n$, whereas we are looking for the current that produces $R \sim R_n$. Further details of the measurement techniques have been published in a previous paper⁷ and other recent papers.^{1,6}

IV. RESULTS AND ANALYSIS

Figure 1(a) shows the resistive transitions at different electric currents I for the medium sample. The inset shows the sample geometry. The horizontal sections of the current leads add a small ($\sim 15\%$) series resistance to the actual resistance of the bridge. Because j in these wide regions is negligible, this resistance freezes out at the nominal unshifted T_c , making the onset seem to not shift. Similarly, the lower foot of the transition will have a flux-motion contribution $R_f \sim R_n B/H_{c2} < 5\% R_n$ from the self-field. The central two-thirds portion of the transitions [magnified in panel (b)] circumvents these errors, displaying relatively parallel shifts due to pair breaking. Variations in film thickness cause the transitions to broaden slightly with increasing j [the functional shape for a simple series model is given by $R(j, T, \delta t) = R_n \{ \ln(j/j_d(0)) - 1.5 \ln(1 - T/T_c) \} / \ln(1 + \delta t/t)$, where δt represents thickness variation]. At the $R_n/2$ criterion (shown by the dashed line) the actual T_c shifts correspond to shifts for a sample with the same mean thickness t but with $\delta t = 0$. Panels (c) and (d) show similar sets of curves for the other two samples. It should be noted that in addition to transition broadening due to thickness variations or inhomogeneity, the $R(T)$ transition may have some intrinsic width as a function of j . An analogous situation arises for $R(T)$ in a magnetic field, where there is an intrinsic broadening as B is increased.⁹ Unfortunately, there is no theoretical work on the $R(T)$ transition shape at high j . Nevertheless, we expect the midpoint criterion for the shifted T_c to provide a factor-of-2 estimate of j_d .

Figure 2(a) shows the midpoint T_c 's and their corresponding currents (ranging from 10^{-6} to $10^{-2}\ \text{A}$) plotted as $I^{2/3}$ (expected for pair breaking) and as I^2 (expected for Joule heating). The shifts are closely proportional $I^{2/3}$ rather than to I^2 , showing that heating is not appreciable (the plots for samples S and L look similar). The slope $dI^{2/3}/dT_c(j)$ together with Eq. (7) gives a zero-temperature depairing current value of $257\ \text{mA}$ (if the T_c criterion is taken at 30% and 70% of R_n , the corresponding I_d values are $196\ \text{mA}$ and $299\ \text{mA}$, respectively). Dividing this by the cross-sectional area

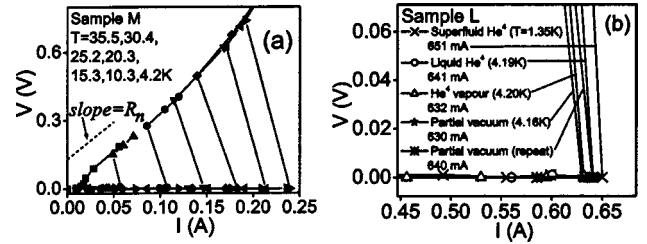


FIG. 3. (a) IV curves for sample M at seven fixed temperatures (listed for curves going from left to right). Beyond j_d , the voltage jumps to a linear behavior reflecting the resistance of the normal state (slope indicated by the dashed line). (b) IV curves for the largest sample in different thermal environments to evaluate Joule heating.

gives a current density of $j_d(0) = 2.1 \times 10^7\ \text{A/cm}^2$. The respective values for samples S and L are $j_d(0) = 2.2 \times 10^7$ and $1.8 \times 10^7\ \text{A/cm}^2$. The three values are consistent within the uncertainties in the sample dimensions, implying a cross-sectionally uniform current density. This is expected for the dissipative state of a superconductor and close to the $T_c(j)$ boundary where λ and ξ (coherence length) diverge [In the fluctuation region near the $T_c(j)$ boundary and during flux motion—when the superconductor is resistive—the current flow becomes macroscopically uniform, as in a normal conductor, due to the principle of minimum entropy production. This has been discussed and verified elsewhere.¹]. Panel (b) of the Fig. 2 shows pulse wave forms at the highest dissipation levels.

Figure 3(a) shows current-voltage (IV) characteristics at various fixed temperatures for sample M (results for samples S and L are similar). As I is increased, V remains close to zero until some critical value. Above this it shows Ohmic behavior $V = IR_n$. Note that at $T = 35.5\ \text{K}$ the transition is gradual, whereas at the lower temperatures it is rather abrupt. This may be in part because a type-II superconducting phase transition changes from second order to first order at lower temperatures in the presence of a current.³ The “s” shape arises because the external circuit feeding the pulsed signal has a source impedance $R_s \approx 12\ \Omega$. Thus when the sample is driven normal, the current will drop discontinuously by the fraction $R_n/(R_n + R_s) \sim 20\%$ as observed.

The relevance of Joule heating was assessed by measuring the IV curves in different thermal environments [the curves of Fig. 3(a) were measured in helium vapor]. Figure 3(b) shows a set of IV curves for the large (L) sample (its lower surface-to-volume ratio makes it most vulnerable to heating) in superfluid, normal liquid, vapor, and vacuum. The absence of a significant systematic influence of the thermal environment shows that Joule heating is not consequential.¹⁰

From such IV characteristics measured at the lowest temperature ($1.5\ \text{K}$) in superfluid helium, the current required to drive the sample normal provides a direct measurement of $j_d(T \approx 0)$. For the three samples S , M , and L , these respective values are $j_d(0) = 1.9 \times 10^7$, 2.0×10^7 , and $1.7 \times 10^7\ \text{A/cm}^2$, which are consistent with the values obtained earlier (2.2×10^7 , 2.1×10^7 , and $1.8 \times 10^7\ \text{A/cm}^2$) from the shifts in the resistive transitions near T_c [Fig. 2 and Eq. (7)].

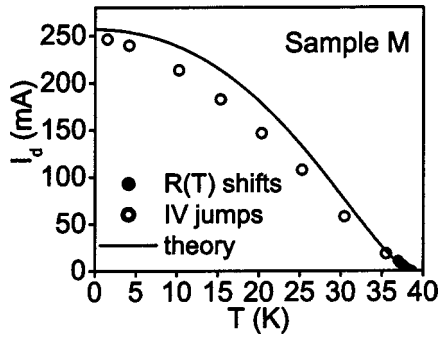


FIG. 4. Pair-breaking currents from IV curves (Fig. 3) and T_c shifts (Figs. 1 and 2). The solid line represents the theoretical curve [Eq. (5)] in which $I_d(0)$ and T_c are fixed by the T_c shifts (Fig. 2; $36 < T < 39$), with no adjustment made over the rest of the range ($1.5 \leq T \leq 36$ K).

It may be reiterated that the measurement does not reflect a depinning j_c ; without significant pair breaking, the motion of the minuscule self-flux ($B \ll H_{c2}$) will produce $R_f \ll R_n$. The observed $R \approx R_n$ is reached only when the current induces pair breaking and drives the system normal. Thus the observed magnitudes of $j_d(0)$ are indeed independent of sample widths and agree with the values projected from the resistive transition shifts.

Figure 4 shows the values of I_d at different temperatures obtained from the IV characteristics of Fig. 3(a). Also shown are the values of I_d obtained from the shifts in the resistive transition near T_c (from Fig. 2). The solid line is a plot of Eq. (5) in which the values of $T_c(0)$ and $I_d(0)$ came directly from the observed $j^{2/3}$ behavior of Fig. 2 and were not adjusted to fit the other data over the extended temperature range, nor was $I_d(0)$ adjusted to fit the actual measured value from the IV characteristic at low T (i.e., Fig. 3). Nevertheless, without adjustments, the $I_d(T)$ data tend to follow the general trend of Eq. (5).

V. CONCLUSIONS

In conclusion, we have studied current-induced pair breaking in magnesium diboride over the entire temperature

range for in-plane current transport. The measured $j_d(T)$ function is consistent with the Ginzburg-Landau form and conforms exactly to the $\Delta T_c \propto j^{2/3}$ behavior predicted near T_c . $j_d(0)$ obtained from the value of current required to drive the sample normal at $T \rightarrow 0$, agrees with the $j_d(0)$ deduced from the $\Delta T_c \propto j^{2/3}$ behavior close to T_c . The average value for all samples by both methods is $j_d(0) \approx 1.9 \pm 0.4 \times 10^7$ A/cm²; besides the $\pm 0.4 \times 10^7$ A/cm² statistical error, there is a systematic error bar of a factor of ~ 2 related to the resistive criterion for $T_c(j)$. Our experimental estimate of $j_d(0)$ is comparable in order of magnitude to the estimate of 6×10^7 A/cm² calculated from Eq. (6) and the published values of $H_c = 2500$ G and $\lambda = 185$ nm from the review on MgB₂ by Wang *et al.*,⁸ considering the uncertainties in those parameters. From a technological standpoint, the depairing current density of MgB₂ is about an order of magnitude lower than the high- T_c cuprates.¹¹ The good news is that the flux pinning in films is so strong (because of the larger coherence length and more isotropically three-dimensional behavior) that the depinning j_c at modest fields appear to be within an order of magnitude of j_d ,¹² whereas for the cuprates j_c and j_d can be separated by two or three orders of magnitude.⁷

The tremendous experimental difficulties against measuring $j_d(0)$ until now, can be appreciated when one sees that for Y₁Ba₂Cu₃O₇ [where $j_d(T \approx T_c)$ was measured¹¹] the power density would be^{1,11} $\rho j^2 \sim 10^{-4} (10^8)^2 \sim 10^{12}$ W/cm³—hopelessly beyond our pulsed technique's limit of $\sim 10^{10}$ W/cm³ (low- T_c materials such as Nb and Pb also have prohibitive ρj^2 values). MgB₂'s parameters [$\rho j^2 \sim 10^{-5} (10^7)^2 \sim 10^9$ W/cm³] brought $j_d(0)$ within experimental reach.

ACKNOWLEDGMENTS

The authors acknowledge useful discussions and other assistance from J. M. Knight, B. I. Ivlev, C. Wu, D. H. Arcos, H. H. Arcos, H. J. Kim, E. M. Choi, K. J. Kim, and D. K. Finnemore. This work was supported by the U. S. Department of Energy through Grant No. DE-FG02-99ER45763 and by the Creative Research Initiatives of the Korean Ministry of Science and Technology.

*URL: <http://www.physics.sc.edu/kunchur>; Electronic address: kunchur@sc.edu

¹M.N. Kunchur, B.I. Ivlev, D.K. Christen, and J.M. Phillips, Phys. Rev. Lett. **84**, 5204 (2000).

²Michael Tinkham, *Introduction to Superconductivity*, 2nd ed. (McGraw-Hill, New York, 1996).

³J. Bardeen, Rev. Mod. Phys. **34**, 667 (1962).

⁴W.N. Kang *et al.*, Science **292**, 1521 (2001).

⁵W.N. Kang *et al.*, Physica C **385**, 24 (2003).

⁶M.N. Kunchur, Phys. Rev. Lett. **89**, 137005 (2002).

⁷M.N. Kunchur, Mod. Phys. Lett. B **9**, 399 (1995).

⁸Y. Wang, T. Plackowski, and A. Junod, Physica C **355**, 179 (2001).

⁹M. Tinkham, Phys. Rev. Lett. **61**, 1658 (1988).

¹⁰O.M. Stoll, S. Kaiser, R.P. Huebener, and M. Naito, Phys. Rev. Lett. **81**, 2994 (2001).

¹¹M.N. Kunchur, D.K. Christen, C.E. Klabunde, and J.M. Phillips, Phys. Rev. Lett. **72**, 752 (1994).

¹²H.-J. Kim *et al.*, Phys. Rev. Lett. **87**, 087002 (2001); S.H. Moon *et al.*, Appl. Phys. Lett. **79**, 2429 (2001); C.B. Eom *et al.*, Nature (London) **411**, 558 (2001).